J Mol Neurosci (2016) 60:71–81
DOI 10.1007/s12031-016-0793-9

Neuroprotective Effect of Osthole on Neuron Synapses in an Alzheimer's Disease Cell Model via Upregulation of MicroRNA-9

Shaoheng Li[1] · Yuhui Yan[1] · Yanan Jiao[1] · Zhong Gao[2] · Yang Xia[3] · Liang Kong[1] · Yingjia Yao[1] · Zhenyu Tao[1] · Jie Song[1] · Yaping Yan[4] · Guangxian Zhang[4] · Jingxian Yang[1]

Received: 4 April 2016 / Accepted: 30 June 2016 / Published online: 9 July 2016

Abstract Accumulation of β-amyloid peptide (Aβ) in the brain plays an important role in the pathogenesis of Alzheimer's disease (AD). It has been reported that osthole exerts its neuroprotective effect on neuronal synapses, but its exact mechanism is obscure. Recently, microRNAs have been demonstrated to play a crucial role in inducing synaptotoxicity by Aβ, implying that targeting microRNAs could be a therapeutic approach of AD. In the present study, we investigated the neuroprotective effects of osthole on a cell model of AD by transducing APP_{695} Swedish mutant (APP_{695}swe, APP) into mouse cortical neurons and human SH-SY5Y cells. In this study, the cell counting kit CCK-8, apoptosis assay, immunofluorescence analysis, enzyme-linked immunosorbent assay (ELISA), quantitative real-time polymerase chain reaction, and Western blot assay were used. We found that osthole could enhance cell viability, prevent cell death, and reverse the reduction of synaptic proteins (synapsin-1, synaptophysin, and postsynaptic density-95) in APP-overexpressed cells, which was attributed to increases in microRNA-9 (miR-9) expression and subsequent decreases in CAMKK2 and p-AMPKα expressions. These results demonstrated that osthole plays a neuroprotective activity role in part through upregulating miR-9 in AD.

✉ Jingxian Yang
jingxian__yang@163.com

[1] School of Pharmacy, Liaoning University of Traditional Chinese Medicine, Dalian, Liaoning 116600, China

[2] Department of Interventional Therapy, Dalian Municipal Central Hospital, Dalian, Liaoning 116033, China

[3] Department of Engineering, University of Oxford, Oxford OX1 3LZ, UK

[4] Department of Neurology, Thomas Jefferson University, Philadelphia, PA 19107, USA

Keywords Osthole · Alzheimer's disease · Amyloid precursor protein · miR-9 · CAMKK2–AMPK pathway · Neuron synapses

Introduction

Alzheimer's disease (AD) is one of the most serious neurodegenerative diseases characterized by progressive cognitive impairment and memory loss and mainly affects people over 65 years old. AD is characterized by extracellular β-amyloid peptide (Aβ) plaques, intracellular neurofibrillary tangles (NFTs), and neuronal synapse loss in the brain (Selkoe 2002; Wilcock et al. 2009; Kudinov et al. 2012; Malthankar-Phatak et al. 2012). Though the pathogenic mechanisms of AD are obscure, the most recognized mechanism is that by which amyloid precursor protein (APP) can be cleaved first by β- and then by γ-secretase generating $Aβ_{1–42}$ oligomers (LeBlanc et al. 1992; Schonrock et al. 2012b), which have strong abilities for inducing neuronal toxicity, synaptic failure, and memory loss in cell or animal models of AD (Selkoe 2002; Haass and Selkoe 2007; Schonrock et al. 2010). Synaptic impairment and synapse loss exist in the early stages of AD (Hawley et al. 1996; Stapleton et al. 1996; Mairet-Coello et al. 2013). Synaptic proteins, synapsin, synaptophysin (SYP), and postsynaptic density-95 (PSD-95), play crucial roles in synapse maturation and plasticity (Stein et al. 2000). It has been reported that soluble Aβ treatment significantly reduced the level of these proteins in rat hippocampal neurons (Carling et al. 2012). Furthermore, $Aβ_{1–42}$ oligomers can induce an acute rapid synaptotoxic effect by activating the CAMKK2–AMPK pathway (Mairet-Coello et al. 2013). However, no effective drugs are currently available for treating neurotoxicity, making it important to develop effective therapeutic agents.

As a natural coumarin derivative isolated from *Cnidium monnieri* (L.) Cusson, osthole (7-methoxy-8-isopentenoxycoumarin, $C_{15}H_{16}O_3$, 244.39 Da; Fig. 1) has recently drawn considerable attention from researchers because of its broad-spectrum pharmacologic attributes, such as anti-inflammatory (Gao et al. 2014; Xia et al. 2015), anti-apoptotic (Hu et al. 2013), anti-oxidative stress (Chen et al. 2011), and anti-tumor (Nakamura et al. 2009) activities. Previous research from the authors of the current study has reported that osthole (50 μmol/L) had no effect on cell survival and apoptosis compared with that of the control. However, osthole had a neuroprotective effect against Aβ injury, promotes neuron survival, and reverses cell death via cyclic AMP response element-binding protein (CREB) phosphorylation (Hu et al. 2013). Moreover, Dong X et al. suggested that osthole may improve learning and memory impairment and increase synaptic plasticity in AD rats via regulating glutamate (Dong et al. 2012).

microRNAs are a recently identified large family of 21–23-nucleotide non-coding RNAs that are involved in numerous cellular processes, including development, proliferation, apoptosis, and synaptic plasticity (Ambros 2004; Chen et al. 2004; Carmell et al. 2007). Among the microRNAs, microRNA-9 (miR-9) is expressed specifically in neurogenic regions of the brain during neural development and in adulthood. Recently, researchers have been investigating in vitro and in vivo reduction of miR-9 (Schonrock et al. 2010; Schonrock et al. 2012a; Che et al. 2014). Moreover, Chang F et al. provided evidence showing that CAMKK2 is a target gene of miR-9 and investigated the role of miR-9 on Aβ1–42-triggered CAMKK2–AMPK activation and synaptotoxicity (Chang et al. 2014).

Based on the aforementioned evidences, this study hypothesized that osthole can perform neuroprotection and rescue the decrease of synaptic proteins in cells stably transduced with APP, and the study aimed to investigate the underlying mechanism of miR-9. The findings of this study demonstrated that osthole exerts its neuroprotective effect on neuron synapses via upregulating miR-9 and subsequently downregulating CAMKK2 and p-AMPKα expressions in APP-overexpressed cells.

Materials and Methods

Generation of Primary Cortical Neurons and SH-SY5Y Cells

Neurons were isolated from the cortices of newborn (0–2 days) mice (C57BL/6) and cultured in special media as described in the laboratory where the study was performed (Hu et al. 2013). Briefly, meninges-free cortices were isolated and cut into pieces of 1 mm^3 and then suspended in 3 mL 0.25 % trypsin–EDTA (Gibco Invitrogen Corporation, NY, USA) at 37 °C for 15 min. The cells (10^6/mL) were plated on poly-L-lysine–coated 24-well plates (BD Bioscience, CA, USA) and maintained at 37 °C in a humidified atmosphere (5 % CO_2, 95 % air). Neurons were cultured in Dulbecco's modified Eagle's medium (DMEM, Gibco) high-glucose media with 10 % fetal bovine serum (FBS, Gibco) and 100 U/mL penicillin and 100 μg/mL streptomycin (1 % P/S, Gibco). The media were replaced with DMEM containing 4 μg/mL cytarabine in 3 days after seeding, which suppressed the growth of gliocytes and consistently provided neuronal cultures with 90 % purity. After 15-day culture, neurons were used in the experiment. The human neuroblastoma cell line SH-SY5Y (Capital Medical University, Beijing, China) was cultured in DMEM/F12 (Gibco) supplemented with 10 % FBS and 1 % P/S at 37 °C in a humidified 5 % CO_2, 95 % air.

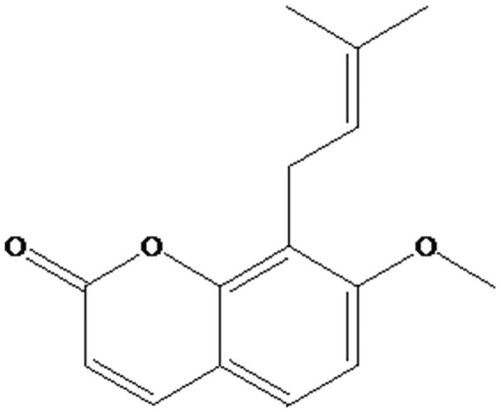

Fig. 1 The chemical structure of osthole

Construction of Lentiviral Vector Encoding APP and GFP and Transduction into Neurons and SH-SY5Y Cells

To generate APP expression construct, the APP sequence (AuGCT DNA-SYN Biotechnology Co. Ltd. Beijing, China) was subcloned into the green fluorescent protein (GFP) lentiviral vector pCDH-CMV-MCS-EF1-copGFP (System Biosciences; CA, USA) at *Xba*I and *Not*I restriction sites (Invitrogen) (Yang et al. 2012). The newly generated APP and three other helper plasmids pLP1, pLP2, and pLP/VSV-G (Invitrogen) were isolated from bacteria using the plasmid small kit without endotoxin (Omega Bio-tek, GA, USA), and their concentrations were adjusted to 1 μg/μL. The 293T cells (Dalian Medical University, Dalian, China) were cultured in DMEM supplemented with 10 % FBS and 1 % P/S. Ninety percent of confluent 293T cells in DMEM were transfected with plasmid DNA containing 15 μg APP or 15 μg GFP (negative control vector), 6.5 μg pLP1, 2.5 μg pLP2, and 3.5 μg pLP/VSV-G using Lipofectamine 2000 (Life Technologies, Gaithersburg, MD, USA) in 10-cm

dishes. After 6 h, the medium with plasmids was replaced by 10-mL fresh culture medium. The culture medium was harvested after 2 days, filtered through a 0.45 μm membrane, and then stored at −80 °C for further use (Yang et al. 2009; Yang et al. 2012; Yang et al. 2014). Viral titers were assayed by infecting 293T cells at different dilutions; titers were adjusted to 5×10^8 IU/mL before infection. Lentiviral particles encoding APP-GFP and GFP were transduced into neurons and SH-SY5Y cells, respectively. After 3 days, the stably transduced cells were determined by immunocytochemistry or cultured for future use.

Preparation of Osthole

Osthole (structure shown in Fig. 1, purity >98 %) was purchased from the National Institute for the Control of Pharmaceutical and Biological Products (110822-200407; Beijing, China). Moreover, 12.2 mg of osthole was dissolved in 10 μL dimethyl sulfoxide (DMSO) and was diluted with 1 ml DMEM or DMEM/F12 to stock solution of 50 mM. APP-overexpressed cells were treated with osthole at a final concentration of 50 μM (the concentration of DMSO was 0.0001 %, which had no effect on neuronal cells) for 24 h (Hu et al. 2013; Gao et al. 2014; Yao et al. 2015). The GFP group was administered with the same concentration of DMSO as the APP group, but without osthole (Zhang et al. 2011; Yao et al. 2015).

Cell Viability Test

Cell viability was assessed using the cell counting kit CCK-8 (Dojindo Laboratories; Kumamoto, Japan) according to the manufacturer's instruction. In brief, 10 μL of CCK-8 solution was added to each well containing 100 μL of cell culture supernatants (10^5 cells) of the 96-well plates (Wu et al. 2014; Xu et al. 2014). The reaction system was incubated at 37 °C for 4 h. The absorbance was measured in a microplate reader (MR-96, Mindray, Shenzhen, China) at 450 nm.

Cell Death Determination

Terminal deoxynucleotidyl transferase-mediated dUTP nick-end labeling (TUNEL) was performed using a one-step assay kit (KeyGen, Nanjing, China). The neurons and SH-SY5Y cells were fixed with 4 % paraformaldehyde for 25 min and penetrated with 1 % Triton X-100 for 5 min. Then, the cells were incubated in the dark with 50-μL TdT solutions for 60 min and streptavidin-TRITC solutions for 30 min at 37 °C according to the manufacturer's protocol (Zhou et al. 2009; Lu et al. 2013). Morphological changes in cells undergoing apoptosis were detected simultaneously by counterstaining them with DAPI (1:100, Sigma, St. Louis, MO, USA). The slides were examined by an inverted fluorescence microscope (Nikon Eclipse E800; Nikon, Tokyo). The experiments were conducted in triplicate.

Immunofluorescence Labeling

Cells in 96-well plates were fixed with 4 % paraformaldehyde, penetrated with 1 % Triton X-100, and then washed three times with phosphate-buffered saline (PBS). Sections were incubated with 10 % goat serum in PBS for 30 min, after which primary antibodies were added and incubated at 4 °C overnight. The following primary antibodies were used: rabbit anti-NF-M (1:150, STEMCELL Technologies, Vancouver, BC, Canada), anti-APP (1:150, Abcam, Cambridge, MA, USA), and anti-synapsin-1 (1:150, Abcam). After washing three times with PBS, the sections were incubated with Cy3-conjugated donkey anti-rabbit immunoglobulin G secondary antibodies (1:200, Jackson, West Grove, PA, USA) for 1 h at room temperature (Hamamoto et al. 2004; Yang et al. 2010; Hu et al. 2013). All of these were then supplemented with DAPI nuclear dye, washed third with PBS, and viewed using an inverted fluorescence microscope. ImageJ (National Institutes of Health, Bethesda, MD, USA) was used for quantitative analysis.

Analysis of Synaptic Protein Levels by Enzyme-Linked Immunosorbent Assay

Neurons and SH-SY5Y cells were cultured (10^6/mL) in 96-well plates. Media were collected and assayed for SYP and PSD-95 using an enzyme-linked immunosorbent assay (ELISA) kit (Jiangsu Kurt Trading Co. Ltd.; Jiangsu, China) according to the manufacturer's instruction.

Quantitative Real-Time Polymerase Chain Reaction

Real-time polymerase chain reaction (RT-PCR) was carried out as previously described (Hu et al. 2013; Lee et al. 2013; Zhang et al. 2013). Total cellular RNA was extracted using TRIzol reagent (Carlsbad, CA, USA) and quantified using a spectrophotometer. RNA (3 μg) was converted to complementary DNA (cDNA) by reverse transcriptase using a Revert Aid First Strand cDNA Synthesis Kit (Thermo Scientific, Lafayette, CO, USA). miR-9 and U6 small nucleolar RNA (Guangzhou RiboBio Co., Ltd., Guangzhou, China) were used for the normalization; U6 snRNA (U6) served as the control. The PCR reaction was performed using 2 μL cDNA and a DreamTaq Green PCR Master Mix Kit (Thermo) as follows: 95 °C for 10 min; 35 cycles of 95 °C for 30 s, 57 °C for 30 s, and 72 °C for 60 s; and 72 °C for 10 min. RT-PCR products were resolved in 4 % agarose gel stained with ethidium bromide. Quantitative analysis was performed using a Tanon 4100

Gel Imaging System (Tanon Science & Technology Co., Shanghai, China).

MiR-9 Inhibitor Transfection

APP-overexpressed cells in DMEM were transfected with antisense miR-9 oligonucleotide (GenePharma, Shanghai, China) using Lipofectamine 2000 reagent according to the manufacturer's instructions (Wang et al. 2011). After 72 h, the cells were subjected to further analysis as described in the "Results" section. We checked miRBase database and found that the sequence of miR-9 in mice is the same as it in human. So, the miR-9 inhibitor can be used in both mouse neurons and human SH-SY5Y cells.

Western Blot Analysis

Proteins were extracted with a ReadyPrep protein extraction kit according to the manufacturer's instructions (R&D, CA, USA) from neurons after osthole treatment for 1 day. Equal amounts of proteins (50 μg) were loaded on 10 % SDS-PAGE and transferred onto polyvinylidene difluoride membranes. The membranes were blocked for 1 h with a blocking buffer containing 5 % BSA in Tris-buffered saline solution and Tween 20 (10 mM Tris–HCl, 150 mM NaCl, 0.05 % Tween 20; TBS-T). The membranes were then incubated overnight at 4 °C with different primary antibodies diluted in the same blocking buffer. Incubations with HRP-conjugated secondary antibodies were performed for 1 h at room temperature and visualized by quantitative chemiluminescence using ECL western blotting detection reagents (Millipore) (Yang et al. 2008; Zhuang et al. 2012) Signal intensity was quantified using ImageJ. Antibodies used were as follows: mouse anti-Aβ1–42 (1: 1500, Abcam), rabbit anti-phospho-T172-AMPKα (1:1000; Cell Signaling), AMPKα (1:1000; Cell Signaling), and anti-CAMKK2 (1:1000; Abcam). To control for loading, blots were stripped and reprobed with mouse anti-actin (1:2000; Santa Cruz).

Statistical Analysis

The data were analyzed using SPSS version 13.0 (SPSS, IL, USA) and were expressed as the means ± standard deviation (SD). Differences for other parameters were evaluated by the analysis of variance (for multiple groups) or Student's test (for two groups). Differences were considered significant at a value of $P < 0.05$.

Results

$A\beta_{1–42}$ Secreted from GFP- and APP-Expressing Cells Exists as a Neurotoxic Oligomer

Neurons and SH-SY5Y cells were identified by immunostaining of neural-specific marker neurofilament M (NF-M). Figure 2 shows that both neurons and SH-SY5Y cells were positive to NF-M. Then, these cells were transduced either with lentiviral vector APP encoding both APP and GFP or with GFP encoding GFP alone (used as control). At day 3 post-transduction, neurons and SH-SY5Y cells that were transduced with lenti-APP-GFP exhibited GFP-positive staining at 95 and 93 %; strong APP staining was visible in neurons and SH-SY5Y cells transduced with APP but not with GFP, while strong GFP expression was visible in cells transduced with both vectors (Fig. 3a, b). The results demonstrated the high efficiency of APP transduction into neurons and SH-SY5Y cells and abundant expression of $A\beta_{1–42}$ (Fig. 3c, d), which acts as a neurotoxic oligomer (Haass and Selkoe 2007; Schonrock et al. 2010).

Osthole Promotes Cell Survival and Reduces Apoptosis in APP-Overexpressed Cells

To study the effect of osthole on cell viability in these cells, neurons and SH-SY5Y cells were incubated with osthole (50 μmol/L) for 24 h (Xu et al. 2011; Hu et al. 2013). Next,

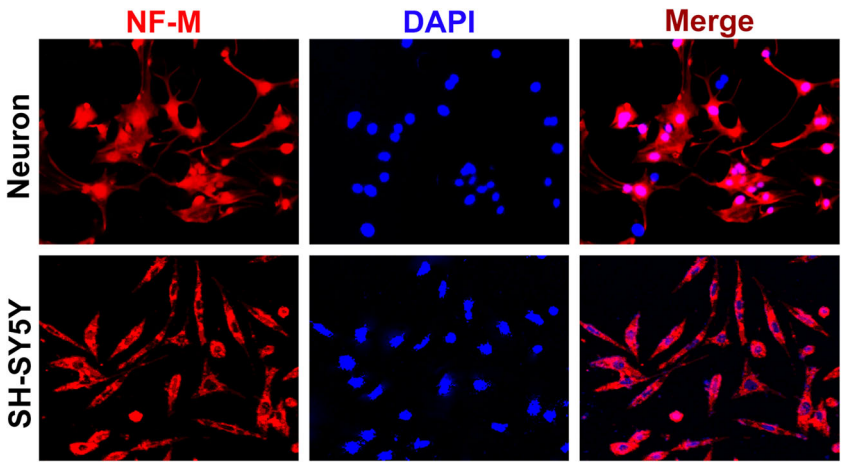

Fig. 2 Characterization of neurons and SH-SY5Y cells by immunostaining. Neurons (**a**) and SH-SY5Y cells (**b**) were identified by immunostaining of neural markers NF-M (*red*) and DAPI (*blue*). *Scale bar* = 25 μm

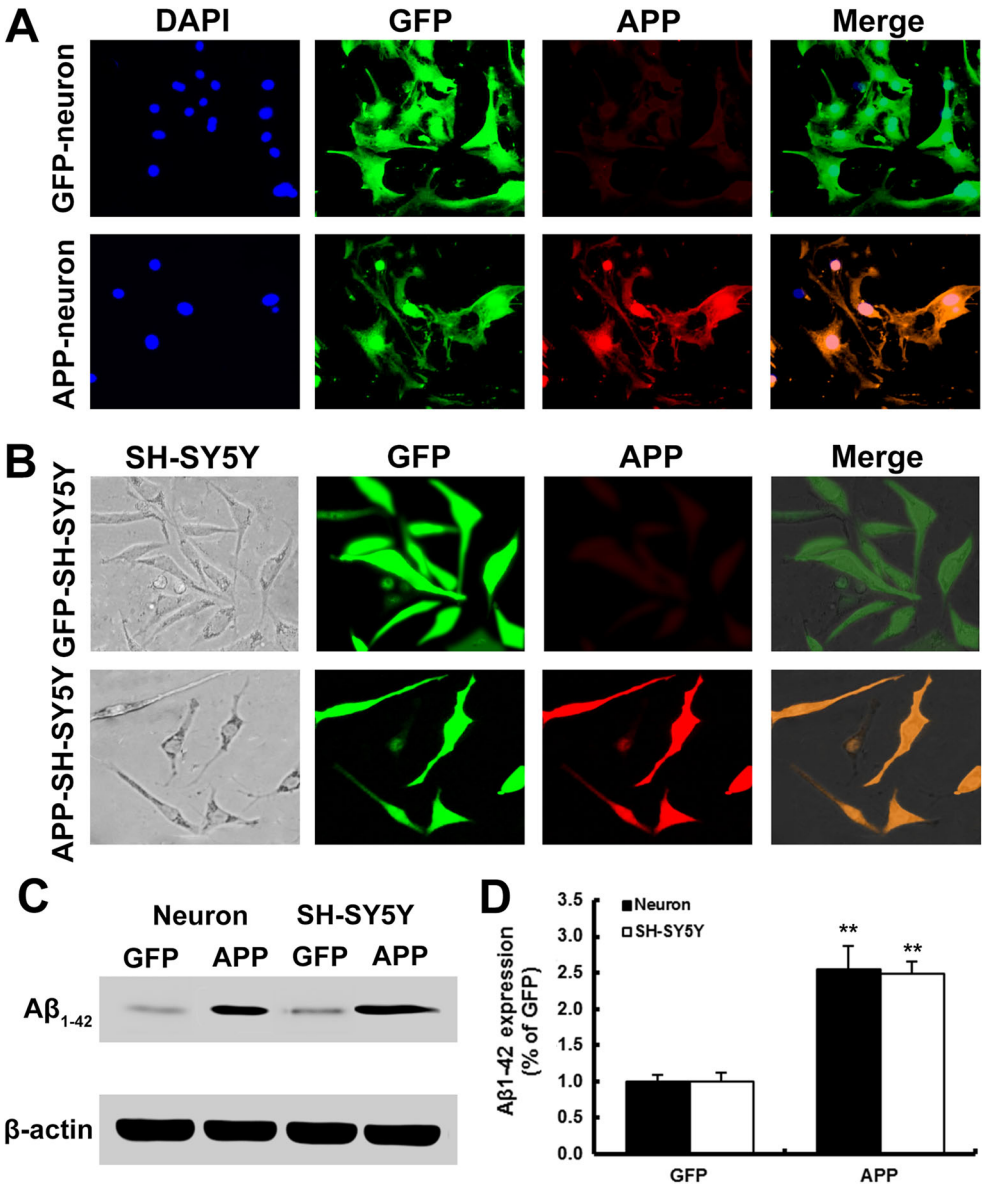

Fig. 3 $A\beta_{1-42}$ secreted from GFP- and APP-expressing cells in culture media. **a** Neurons transduced with both vectors are GFP^+ and exhibit neural cell morphology. APP (*red*) was expressed in APP neurons but not in GFP neurons; nuclei were stained with DAPI (*blue*). *Scale bar* = 20 μm. **b** SH-SY5Y cells transduced with both vectors are GFP^+ and exhibit neural cell morphology. APP (*red*) was expressed in APP-SH-SY5Y but not in GFP-SH-SY5Y. *Scale bar* = 20 μm. **c** APP-transduced cells transcribed highly expressed $A\beta_{1-42}$ proteins. **d** Quantitative analysis of $A\beta_{1-42}$ protein level. $^{**}P < 0.01$, vs. GFP groups

the cell viability was assessed using the CCK-8 kit. As shown in Fig. 4a, a significant decline in neural viability was demonstrated in APP-overexpressed neurons and SH-SY5Y cells (60.00 ± 2.48 and 70.57 ± 5.59 %, respectively) of the GFP group (Fig. 4a, $^{**}P < 0.01$, $^{**}P < 0.01$, vs. GFP group 100 %). However, osthole significantly increased the viability to (88.10 ± 6.57 %) and (90.24 ± 6.41 %), respectively (Fig. 4a, $\#\#P < 0.01$, $\#\#P < 0.01$, vs. APP group).

Apoptotic cells were further assessed using the TUNEL assay. The results indicated that cells transduced with APP increased the rate of TUNEL-positive cells (red) to 37.20 ± 2.56 % in neurons ($^{**}P < 0.01$, compared with the GFP neuron group) and 40.00 ± 2.16 % in SH-SY5Y cells ($^{**}P < 0.01$, compared with the GFP-SHSY5Y group). Meanwhile, the percentages of apoptotic cells were 18.29 ± 1.78 % in neurons ($\#\#P < 0.01$, compared with the APP neuron group) and 20.73 ± 1.75 % in SH-SY5Y cells cultured with osthole ($\#\#P < 0.01$, compared with the APP-SHSY5Y group) (Fig. 4b, c).

Osthole Increased miR-9 Expression in APP-Overexpressed Cells

To investigate whether osthole treatment could regulate the expression of miR-9 in APP-overexpressed cells, microRNA (miRNA) RT-PCR assay was used. In this study, APP transduction led to the inhibition of miR-9 expression in neurons and SH-SY5Y cells. In contrast, osthole treatment resulted in the upregulation of miR-9 (0.60 ± 0.05 % APP + Ost group vs. 0.40 ± 0.03 APP group in neurons, $P < 0.01$; 0.61 ± 0.05 APP + Ost group vs. 0.41 ± 0.01 % APP group in SH-SY5Y cells, $P < 0.01$; Fig. 5a, b).

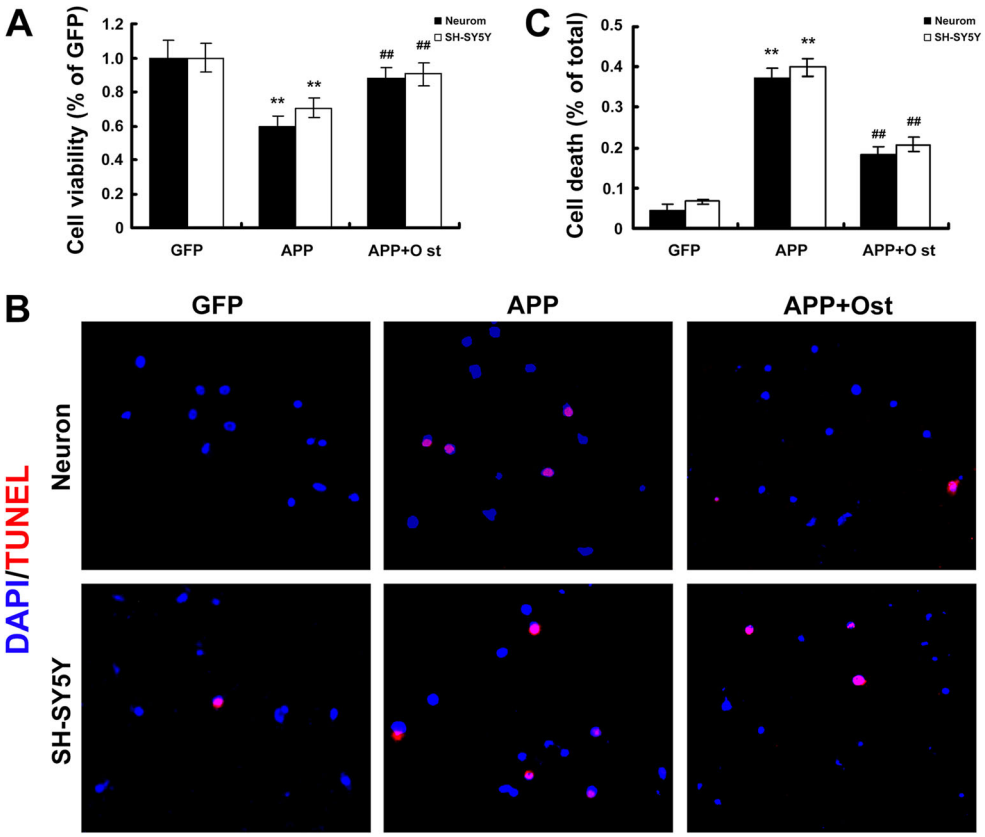

Fig. 4 Osthole enhances the viability of APP-transfected cells and decreases the number of apoptotic cells. **a** Cell viability was assessed by CCK-8 assay. $^{**}P < 0.01$ vs. GFP, $^{\#\#}P < 0.01$ vs. APP alone. **b** Immunocytochemistry staining showed that apoptotic neurons (*upper*) and SH-SY5Y cells (*lower*) were stained by TUNEL (*red*); nuclei were stained by DAPI (*blue*). *Scale bar* = 25 μm. **c** Quantification of the percentage of apoptotic cells. $^{**}P < 0.01$ vs. GFP, $^{\#\#}P < 0.01$ vs. APP alone. The data are expressed as the mean ± SD and represent three independent experiments

Osthole Inhibited Synapsin-1 Reduction in APP-Overexpressed Neurons

In neurons, an analysis of immunocytochemical staining of synapsin-1, an integral membrane glycoprotein of synaptic vesicles, was performed. Synapsin-1 has been widely used as a synaptic marker to investigate synaptic reinnervation and synaptogenesis (Li et al. 2002). The synapsin-1 expression was measured by immunocytochemistry. Figure 6a shows that synapsin-1 protein strongly expressed in GFP neurons, while the intensity of synapsin-1 decreased in APP neurons (Fig. 6a, b, 57.0 vs. 100 % in GFP neurons, $P < 0.01$); treatment with Ost attenuated the reduction of synapsin-1 and restored the protein obviously (Fig. 6a, b, 81.0 vs. 57.0 % in APP neurons, $P < 0.01$). Meanwhile, to inhibit the function of miR-9, antisense miR-9 oligonucleotide was used. As shown in Fig. 6a, b, miR-9 inhibitor significantly reduced the intensity of synapsin-1 (52.3 vs. 100 % in GFP neurons, $P < 0.01$), while treatment with osthole can reveal the effect of the inhibitor (66.0 vs. 52.3 % in APP neurons, $P < 0.05$).

Osthole Upregulated the Concentration of PSD-95 and SYP in APP-Overexpressed Cells

To further investigate the effect of osthole on neurons synapses, ELISA was used to analyze the concentration of PSD-95 and SYP. The results in the present study (Fig. 6c, d) indicated that the protein levels of PSD-95 and SYP significantly decreased by APP transduction ($P < 0.01$, compared with the two GFP groups), which was significantly reversed by treatment with osthole in neurons and SH-SY5Y cells ($P < 0.01$, compared with the two APP groups). Meanwhile, quantitative analysis showed that cells transfected with miR-9 inhibitor had a significant decrease in the concentration of synaptic proteins compared with GFP groups. The concentration of synaptic proteins had a similar trend of reduction in neurons and SH-SY5Y cells transfected with miR-9 inhibitor ($P < 0.01$, compared with the two GFP groups) and an increase in cells transfected with miR-9 inhibitor plus osthole ($P < 0.01$, compared with the two APP groups).

Osthole Attenuates APP Transduction-Induced Synaptotoxicity via Inhibiting CAMKK2 and p-AMPKα Expressions

Previous studies demonstrated that miR-9 can rescue Aβ42-induced synaptotoxicity by inhibiting the CAMKK2–AMPK pathway (Mairet-Coello et al. 2013). Western blot analysis was carried out to verify the levels of CAMKK2, pT172-AMPKα, and AMPKα protein expressions in the neurons. Figure 7a, b shows that the infection of APP significantly increased the protein levels of CAMKK2 and pT172-

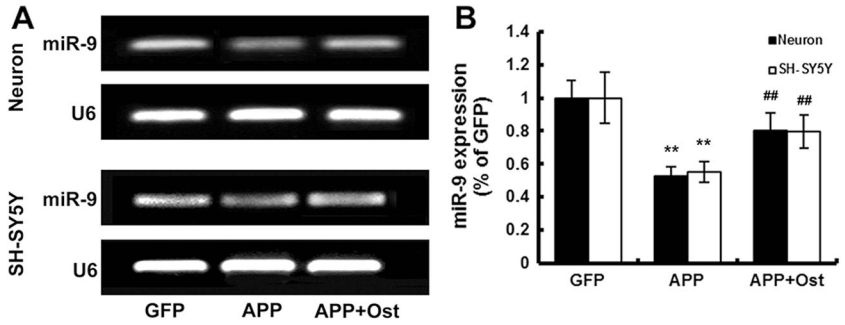

Fig. 5 Osthole treatment increases miR-9 in APP-transfected cells. **a** The expression of miR-9 was detected by RT-PCR in neurons (*upper*) and SH-SY5Y cells (*lower*) after osthole treatment. U6 was included as a loading control. **b** The relative optical density of miR-9 mRNA was acquired by ImageJ. $^{**}P < 0.01$ vs. GFP, $^{\#\#}P < 0.01$ vs. APP alone

AMPKα compared with the GFP group by 124.61 ± 9.10 % ($P < 0.01$) and 168.91 ± 8.47 % ($P < 0.01$) and did not affect the level of total AMPKα ($P > 0.05$). Meanwhile, treatment with osthole reduced the protein levels of CAMKK2 and pT172-AMPKα by 106.99 ± 9.07 % ($P < 0.05$) and 138.97 ± 4.64 % ($P < 0.01$). Inhibition of miR-9 led to an

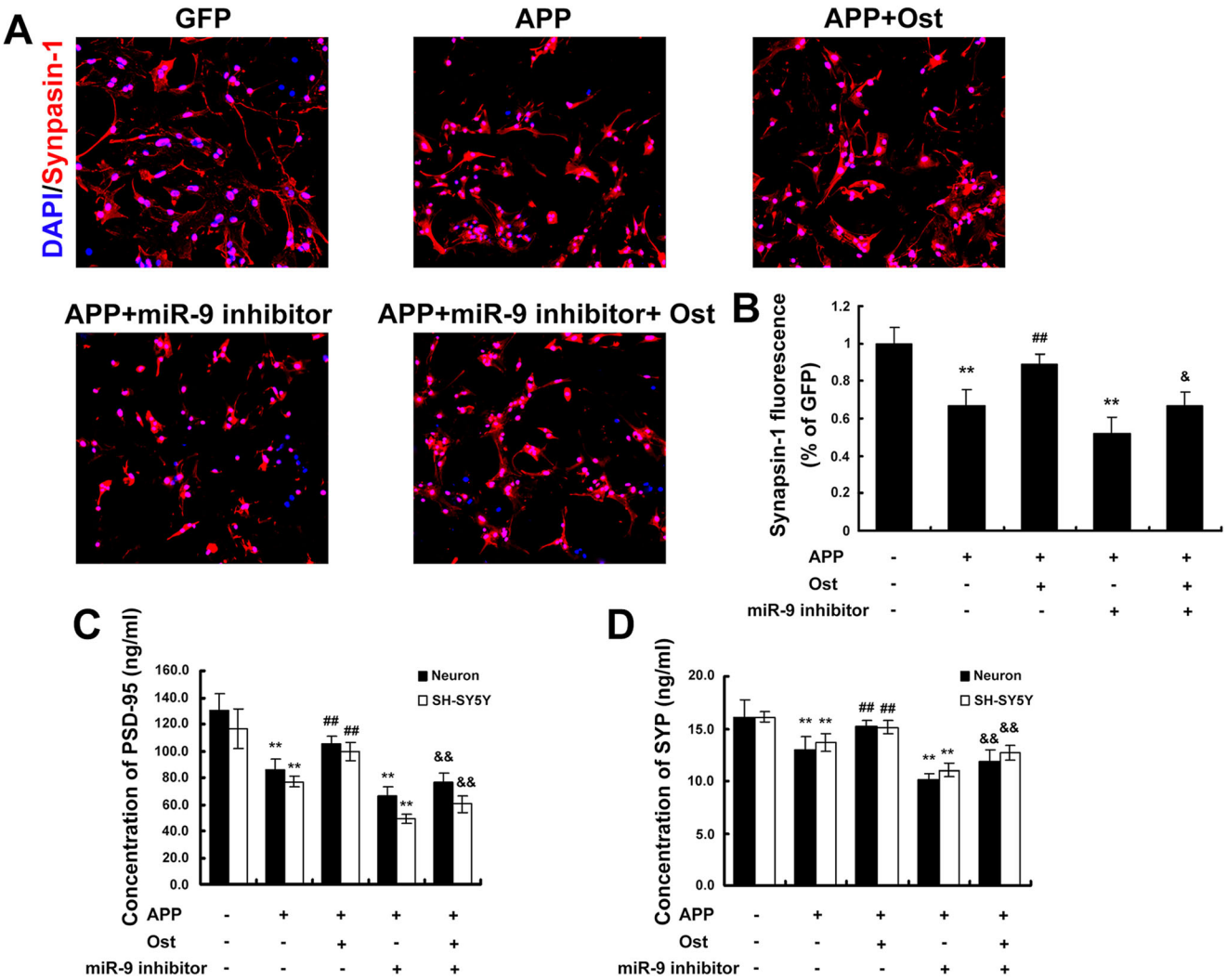

Fig. 6 Osthole protects against APP transfection-induced reduction of synaptic proteins via miR-9 in cells. **a** Immunocytochemistry for synapsin-1 (*red*) and DAPI (*blue*) in neurons. *Scale bar* = 50 μm. **b** Quantification of the synapsin-1 immunoflurescence intensity. PSD-95 (**c**) and SYP (**d**) concentrations measured by ELISA assay. $^{**}P < 0.01$ vs. GFP, $^{\#\#}P < 0.01$ vs. APP alone, $\&P < 0.05$, $\&\&P < 0.01$ vs. APP plus miR-9 inhibitor. Data are expressed as the mean ± SD and represent three independent experiments

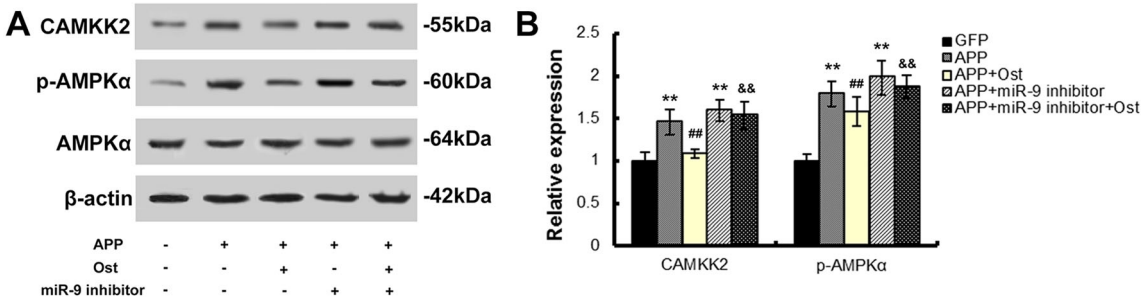

Fig. 7 Effects of osthole and miR-9 on CAMKK2–AMPK pathway expression. **a** Protein levels of CAMKK2, p-AMPKα, and AMPKα in neurons detected by western blotting after osthole treatment or miR-9 inhibitor transfection or the combination. **b** Quantification of protein expression using ImageJ and normalization with β-actin internal control. $^{**}P < 0.01$ vs. GFP, $^{\#\#}P < 0.01$ vs. APP alone, $\&\&P < 0.01$ vs. APP plus miR-9 inhibitor

increase in the levels of endogenous CAMKK2 and pT172-AMPKα proteins compared with the control ($P < 0.01$), while treatment with osthole significantly reduced the endogenous proteins compared with the APP plus miR-9 inhibitor group ($P < 0.01$). These results suggest that osthole exerts its neuroprotective effects partly through upregulation of miR-9 and subsequent downregulation of CAMKK2 and p-AMPKα in APP-overexpressed cells.

Discussion

The role of APP was investigated in neural stem cells and human neuroblastoma cell lines La-N-1 and SH-SY5Y (LeBlanc et al. 1992; Zhang et al. 2011; Lee et al. 2013). Some studies have shown that gene duplications in the APP locus located on chromosome 21 can cause familial AD. Moreover, polymorphisms in the APP promoter, which increases APP transcription that results in elevated Aβ1–42, have been associated with AD (Podlisny et al. 1987; Rovelet-Lecrux et al. 2006; Theuns et al. 2006). In this study, mouse cortical neurons and human neuroblastoma cell line SH-SY5Y were stably transduced with a vector carrying a fragment of APPswe cDNA, which can mimic the characteristics of AD (Fig. 3a, b). After 3 days, $A\beta_{1-42}$ secreted from APP-overexpressed cells existed as a neurotoxic oligomer (Fig. 3c, d), similar to previous reports (Lee et al. 2013).

Osthole, an effective monomer in Chinese medicinal plants, not only can cross the blood–brain barrier and protect against brain injury with its anti-inflammatory and anti-apoptotic effects (Hu et al. 2013; Gao et al. 2014) but also can promote neuron survival and reverse cell death. Herein, it was first demonstrated that APP-overexpressed cells reduced cell viability and increased cell death; second, osthole increased cell viability and significantly inhibited the percentage of TUNEL-positive cells (Fig. 4a–c).

The potential functions of miRNAs acting locally on neuronal synapses are just beginning to be explored (Chen et al. 2004). Several miRNAs are found to be localized and function in dendrites and synapses. Among them, miR-9 is enriched in neurogenic regions of the brain. miR-9 not only promotes the development and differentiation of neurons but also regulates synaptic growth. For example, miR-9 suppresses the expression of target genes to negatively regulate neural stem cell proliferation and accelerate neural differentiation, such as TLX, Foxg1, and hes1 (Podlisny et al. 1987; Shibata et al. 2008; Zhao et al. 2009; Bonev et al. 2012). Ramachandran et al. found that miR-9 overexpression retards tau production in the early stages of AD by inhibiting SIRT1 (Ramachandran et al. 2011). Che and colleagues demonstrated that miR-9 was significantly decreased in both the hippocampus and the forebrain cortex of middle-aged rats when compared to young rats (Che et al. 2014). However, Liu found that miR-9 expression was first slightly downregulated but became markedly increased at 12 weeks in late-onset AD rabbits (Liu et al. 2014). The study revealed that the expression of miR-9 was changed in the different regions of the brain during different disease states (Delay et al. 2012). In a recent report, after interacting with Aβ, miR-9 expression was reduced in neuronal cells, resulting in the increased incorporation of tau and neurofilament H into NFTs (Schonrock et al. 2010). In our study, we also found that the expression of miR-9 in APP-overexpressed cells was decreased, a finding that is consistent with previous studies. Furthermore, osthole significantly increased the expression of miR-9 in APP-overexpressed cells, suggesting that osthole could be a potential agent for treating AD through modulating miR-9 expression (Fig. 5).

Synaptic impairment and synapse loss have been found in the brains of AD patients (Heredia et al. 2006; Um and Strittmatter 2013). Synapses are functional connections between neurons and biological signals and pass information from the presynaptic membrane to the postsynaptic membrane (Ma et al. 2015). Synapsin-1 and SYP, located in the presynaptic membrane, are specific proteins associated with synaptic vesicles that mainly regulate the release of neurotransmitters; PSD-95 is the major scaffolding protein at excitatory synapses and in postsynaptic densities and plays a broad role in plasticity of synaptic structure and function (Chi et al. 2003; Sheng

and Hoogenraad 2007; Woods et al. 2011). Chen et al. showed that solute Aβ treatment significantly reduced synapsin-1 and PSD-95 at synapses in vitro (Chen et al. 2014). Moreover, Jiang et al. showed a decrease of synapse-associated proteins in aging mice (Jiang et al. 2015). The findings of this study also showed a decrease in the expressions of synapsin-1, SYP, and PSD-95 in cortical neurons and human SH-SY5Y cells by APP transduction (Fig. 6). However, treatment with osthole upregulates the expression of the three synaptic proteins (Fig. 6). It confirmed that osthole could enhance synaptic plasticity by increasing these synaptic proteins in APP-overexpressed cells.

AMPK, an important protein kinase in animals and plants, maintains energy homeostasis. It is also a pivotal protein involved in many cellular signaling cascades. This protein is expressed in most cells and is activated by various metabolic stresses such as cell pressure, ischemia, and hypoxia (Culmsee et al. 2001; Vingtdeux et al. 2011). In the mammalian adult brain, AMPK is predominantly expressed in hypothalamic, cortical, and hippocampal neurons. AMPK has three subunits (α, β, and γ), among which, the α subunit has two different isoforms (α1 and α2). The AMPK-α1 subunit is predominantly expressed in the cytoplasm, whereas the α2 subunit is located mainly in the nucleus. At present, the α subunit contains a conserved threonine (Thr-172) site, which is essential for its kinase activity (Ju et al. 2011). Recently, Vingtdeux et al. showed that activated AMPK is abnormally and massively accumulated in pre-tangle- and tangle-containing neurons in AD (Vingtdeux et al. 2011). CAMKK2, one of miR-9 targets, plays an important role in AMPK activation via the phosphorylation of Thr-172 (Chang et al. 2014). Recent research has suggested that Aβ oligomers may disrupt calcium homeostasis, causing a Ca^{2+} influx into cells. It can induce CAMKK2–AMPK pathway activation and lead to synapse loss (Mairet-Coello et al. 2013). However, the overexpression of miR-9 may rescue Aβ42-induced synapse loss by targeting CAMKK2. The findings of the present study demonstrate that the activation of CAMKK2–AMPK pathway induced by APP transduction leads to synapse instability (Fig. 6). However, osthole may protect synaptic functions via upregulation of miR-9 and subsequent downregulation of CAMKK2 and may also inhibit its downstream effects in APP-overexpressed cells (Fig. 7).

To further investigate whether the protective effects of osthole on neuronal synapses depend on the upregulation of miR-9, miR-9 inhibitor was used to inhibit the function of miR-9. The results of this study showed that miR-9 inhibitor inhibited the expression of synaptic proteins (synapsin-1, PSD-95, and SYP) in both APP-transduced neurons and SH-SY5Y cells ($P < 0.01$, Fig. 6), accompanied by the increase in CAMKK2 and pT172-AMPKα expressions in these cells ($P < 0.01$, Fig. 7). Osthole partially reversed the reduction of synaptic proteins, accompanied by the reduction of CAMKK2 and pT172-AMPKα expressions ($P < 0.01$, Figs. 6 and 7). These observations confirmed that the neuroprotective effect of osthole is attributed to the increase in miR-9 expression.

In conclusion, the collective evidence indicates that osthole can promote cell survival and reduce apoptosis in neural cells by APP transduction. Osthole also reversed the reduction of synaptic proteins (synapsin-1, SYP, and PSD-95) in APP-overexpressed cells. Finally, osthole was shown to antagonize the APP transduction-induced synaptotoxic effect by upregulating miR-9 and downregulating CAMKK2 and p-AMPKα, which may be considered as a potential drug in treating AD and other neurodegenerative diseases.

Conclusion

This study demonstrated the neuroprotective effect of osthole in neural cells by APP transduction, and it also highlighted that osthole may contribute to the treatment of some neurodegenerative diseases.

Acknowledgments This work was supported by the National Natural Science Foundation of China (Grant No. 81173580).

Compliance with Ethical Standards

Conflict of Interest The authors declare that they have no conflict of interest.

References

Ambros V (2004) The functions of animal microRNAs. Nature 431:350–355

Bonev B, Stanley P, Papalopulu N (2012) MicroRNA-9 modulates Hes1 ultradian oscillations by forming a double-negative feedback loop. Cell Rep 2:10–18

Carling D, Thornton C, Woods A, et al. (2012) AMP-activated protein kinase: new regulation, new roles? Biochem J 445:11–27

Carmell MA, Girard A, van de Kant HJ, et al. (2007) MIWI2 is essential for spermatogenesis and repression of transposons in the mouse male germline. Dev Cell 12:503–514

Chang F, Zhang LH, Xu WP, et al. (2014) microRNA-9 attenuates amyloidbeta-induced synaptotoxicity by targeting calcium/calmodulin-dependent protein kinase kinase 2. Mol Med Rep 9:1917–1922

Che H, Sun LH, Guo F, et al. (2014) Expression of amyloid-associated miRNAs in both the forebrain cortex and hippocampus of middle-aged rat. Cell Physiol Biochem 33:11–22

Chen CZ, Li L, Lodish HF, et al. (2004) MicroRNAs modulate hematopoietic lineage differentiation. Science 303:83–86

Chen T, Liu W, Chao X, et al. (2011) Neuroprotective effect of osthole against oxygen and glucose deprivation in rat cortical neurons: involvement of mitogen-activated protein kinase pathway. Neuroscience 183:203–211

Chen Y, Wang B, Liu D, et al. (2014) Hsp90 chaperone inhibitor 17-AAG attenuates Abeta-induced synaptic toxicity and memory impairment. J Neurosci 34:2464–2470

Chi P, Greengard P, Ryan TA (2003) Synaptic vesicle mobilization is regulated by distinct synapsin I phosphorylation pathways at different frequencies. Neuron 38:69–78

Culmsee C, Monnig J, Kemp BE, et al. (2001) AMP-activated protein kinase is highly expressed in neurons in the developing rat brain and promotes neuronal survival following glucose deprivation. J Mol Neurosci 17:45–58

Delay C, Mandemakers W, Hébert SS (2012) MicroRNAs in Alzheimer's disease. Neurobiol Dis 46:285–290

Dong X, Zhang D, Zhang L, et al. (2012) Osthole improves synaptic plasticity in the hippocampus and cognitive function of Alzheimer's disease rats via regulating glutamate. Neural Regen Res 7:2325–2332

Gao Z, Wen Q, Xia Y, et al. (2014) Osthole augments therapeutic efficiency of neural stem cells-based therapy in experimental autoimmune encephalomyelitis. J Pharmacol Sci 124:54–65

Haass C, Selkoe DJ (2007) Soluble protein oligomers in neurodegeneration: lessons from the Alzheimer's amyloid beta-peptide. Nat Rev Mol Cell Biol 8:101–112

Hamamoto R, Furukawa Y, Morita M, et al. (2004) SMYD3 encodes a histone methyltransferase involved in the proliferation of cancer cells. Nat Cell Biol 6:731–740

Hawley SA, Davison M, Woods A, et al. (1996) Characterization of the AMP-activated protein kinase kinase from rat liver and identification of threonine 172 as the major site at which it phosphorylates AMP-activated protein kinase. J Biol Chem 271:27879–27887

Heredia L, Helguera P, de Olmos S, et al. (2006) Phosphorylation of actin-depolymerizing factor/cofilin by LIM-kinase mediates amyloid beta-induced degeneration: a potential mechanism of neuronal dystrophy in Alzheimer's disease. J Neurosci 26:6533–6542

Hu Y, Wen Q, Liang W, et al. (2013) Osthole reverses beta-amyloid peptide cytotoxicity on neural cells by enhancing cyclic AMP response element-binding protein phosphorylation. Biol Pharm Bull 36:1950–1958

Jiang Y, Liu Y, Zhu C, et al. (2015) Minocycline enhances hippocampal memory, neuroplasticity and synapse-associated proteins in aged C57 BL/6 mice. Neurobiol Learn Mem 121:20–29

Ju TC, Chen HM, Lin JT, et al. (2011) Nuclear translocation of AMPK-alpha1 potentiates striatal neurodegeneration in Huntington's disease. J Cell Biol 194:209–227

Kudinov AR, Kudinova NV, Kezlia EV, et al. (2012) Compensatory mechanisms to heal neuroplasticity impairment under Alzheimer's disease neurodegeneration. I: the role of amyloid beta and its' precursor protein. Biomed Khim 58:385–399

LeBlanc AC, Kovacs DM, Chen HY, et al. (1992) Role of amyloid precursor protein (APP): study with antisense transfection of human neuroblastoma cells. J Neurosci Res 31:635–645

Lee IS, Jung K, Kim IS, et al. (2013) Amyloid-beta oligomers regulate the properties of human neural stem cells through GSK-3beta signaling. Exp Mol Med 45:e60

Li S, Reinprecht I, Fahnestock M, et al. (2002) Activity-dependent changes in synaptophysin immunoreactivity in hippocampus, piriform cortex, and entorhinal cortex of the rat. Neuroscience 115:1221–1229

Liu QY, Chang MN, Lei JX, et al. (2014) Identification of microRNAs involved in Alzheimer's progression using a rabbit model of the disease. Am J Neurodegener Dis 3:33–44

Lu Y, Xu Y, Yin Z, et al. (2013) Chondrocyte migration affects tissue-engineered cartilage integration by activating the signal transduction pathways involving Src, PLCgamma1, and ERK1/2. Tissue Eng Part A 19:2506–2516

Ma L., Li Y., Wang R. (2015) Drebrin and cognitive impairment. Clin Chim Acta.

Mairet-Coello G, Courchet J, Pieraut S, et al. (2013) The CAMKK2-AMPK kinase pathway mediates the synaptotoxic effects of Abeta oligomers through Tau phosphorylation. Neuron 78:94–108

Malthankar-Phatak GH, Lin YG, Giovannone N, et al. (2012) Amyloid deposition and advanced age fails to induce Alzheimer's type progression in a double knock-in mouse model. Aging Dis 3:141–155

Nakamura T, Kodama N, Arai Y, et al. (2009) Inhibitory effect of oxycoumarins isolated from the Thai medicinal plant Clausena guillauminii on the inflammation mediators, iNOS, TNF-alpha, and COX-2 expression in mouse macrophage RAW 264.7. J Nat Med 63:21–27

Podlisny MB, Lee G, Selkoe DJ (1987) Gene dosage of the amyloid beta precursor protein in Alzheimer's disease. Science 238:669–671

Ramachandran D, Roy U, Garg S, et al. (2011) Sirt1 and mir-9 expression is regulated during glucose-stimulated insulin secretion in pancreatic beta-islets. FEBS J 278:1167–1174

Rovelet-Lecrux A, Hannequin D, Raux G, et al. (2006) APP locus duplication causes autosomal dominant early-onset Alzheimer disease with cerebral amyloid angiopathy. Nat Genet 38:24–26

Schonrock N, Humphreys DT, Preiss T, et al. (2012a) Target gene repression mediated by miRNAs miR-181c and miR-9 both of which are down-regulated by amyloid-beta. J Mol Neurosci 46:324–335

Schonrock N, Ke YD, Humphreys D, et al. (2010) Neuronal microRNA deregulation in response to Alzheimer's disease amyloid-beta. PLoS One 5:e11070

Schonrock N, Matamales M, Ittner LM, et al. (2012b) MicroRNA networks surrounding APP and amyloid-beta metabolism—implications for Alzheimer's disease. Exp Neurol 235:447–454

Selkoe DJ (2002) Alzheimer's disease is a synaptic failure. Science 298: 789–791

Sheng M, Hoogenraad CC (2007) The postsynaptic architecture of excitatory synapses: a more quantitative view. Annu Rev Biochem 76: 823–847

Shibata M, Kurokawa D, Nakao H, et al. (2008) MicroRNA-9 modulates Cajal-Retzius cell differentiation by suppressing Foxg1 expression in mouse medial pallium. J Neurosci 28:10415–10421

Stapleton D, Mitchelhill KI, Gao G, et al. (1996) Mammalian AMP-activated protein kinase subfamily. J Biol Chem 271:611–614

Stein SC, Woods A, Jones NA, et al. (2000) The regulation of AMP-activated protein kinase by phosphorylation. Biochem J 345(Pt 3): 437–443

Theuns J, Brouwers N, Engelborghs S, et al. (2006) Promoter mutations that increase amyloid precursor-protein expression are associated with Alzheimer disease. Am J Hum Genet 78:936–946

Um JW, Strittmatter SM (2013) Amyloid-beta induced signaling by cellular prion protein and Fyn kinase in Alzheimer disease. Prion 7:37–41

Vingtdeux V, Davies P, Dickson DW, et al. (2011) AMPK is abnormally activated in tangle- and pre-tangle-bearing neurons in Alzheimer's disease and other tauopathies. Acta Neuropathol 121:337–349

Wang J, Gu Z, Ni P, et al. (2011) NF-kappaB P50/P65 hetero-dimer mediates differential regulation of CD166/ALCAM expression via interaction with micoRNA-9 after serum deprivation, providing evidence for a novel negative auto-regulatory loop. Nucleic Acids Res 39:6440–6455

Wilcock DM, Gharkholonarehe N, Van Nostrand WE, et al. (2009) Amyloid reduction by amyloid-beta vaccination also reduces mouse tau pathology and protects from neuron loss in two mouse models of Alzheimer's disease. J Neurosci 29:7957–7965

Woods GF, Oh WC, Boudewyn LC, et al. (2011) Loss of PSD-95 enrichment is not a prerequisite for spine retraction. J Neurosci 31:12129–12138

Wu X, Wang Z, Li X, et al. (2014) In vitro and in vivo activities of antimicrobial peptides developed using an amino acid-based activity prediction method. Antimicrob Agents Chemother 58:5342–5349

Xia Y, Kong L, Yao Y, et al. (2015) Osthole confers neuroprotection against cortical stab wound injury and attenuates secondary brain injury. J Neuroinflammation 12:155

Xu SY, Hu YF, Li WP, et al. (2014) Intermittent hypothermia is neuroprotective in an in vitro model of ischemic stroke. Int J Biol Sci 10: 873–881

Xu X, Zhang Y, Qu D, et al. (2011) Osthole induces G2/M arrest and apoptosis in lung cancer A549 cells by modulating PI3K/Akt pathway. J Exp Clin Cancer Res 30:33

Yang J, Bridges K, Chen KY, et al. (2008) Riluzole increases the amount of latent HSF1 for an amplified heat shock response and cytoprotection. PLoS One 3:e2864

Yang J, Jiang Z, Fitzgerald DC, et al. (2009) Adult neural stem cells expressing IL-10 confer potent immunomodulation and remyelination in experimental autoimmune encephalitis. J Clin Invest 119:3678–3691

Yang J, Yan Y, Ciric B, et al. (2010) Evaluation of bone marrow- and brain-derived neural stem cells in therapy of central nervous system autoimmunity. Am J Pathol 177:1989–2001

Yang J, Yan Y, Ma CG, et al. (2012) Accelerated and enhanced effect of CCR5-transduced bone marrow neural stem cells on autoimmune encephalomyelitis. Acta Neuropathol 124:491–503

Yang J, Yan Y, Xia Y, et al. (2014) Neurotrophin 3 transduction augments remyelinating and immunomodulatory capacity of neural stem cells. Mol Ther 22:440–450

Yao Y, Gao Z, Liang W, et al. (2015) Osthole promotes neuronal differentiation and inhibits apoptosis via Wnt/beta-catenin signaling in an Alzheimer's disease model. Toxicol Appl Pharmacol 289:474–481

Zhang N, Wen Q, Ren L, et al. (2013) Neuroprotective effect of arctigenin via upregulation of P-CREB in mouse primary neurons and human SH-SY5Y neuroblastoma cells. Int J Mol Sci 14:18657–18669

Zhang X, Yin WK, Shi XD, et al. (2011) Curcumin activates Wnt/beta-catenin signaling pathway through inhibiting the activity of GSK-3beta in APPswe transfected SY5Y cells. Eur J Pharm Sci 42:540–546

Zhao C, Sun G, Li S, et al. (2009) A feedback regulatory loop involving microRNA-9 and nuclear receptor TLX in neural stem cell fate determination. Nat Struct Mol Biol 16:365–371

Zhou LL, Hou FF, Wang GB, et al. (2009) Accumulation of advanced oxidation protein products induces podocyte apoptosis and deletion through NADPH-dependent mechanisms. Kidney Int 76:1148–1160

Zhuang P, Zhang Y, Cui G, et al. (2012) Direct stimulation of adult neural stem/progenitor cells in vitro and neurogenesis in vivo by salvianolic acid B. PLoS One 7:e35636